Organic & Biomolecular Chemistry

Synthesis of LNA gapmers that replace a phosphorothioate linkage with a sulfonamide in the gap region, and their ability to form duplexes with complementary RNA targets

Journal:	*Organic & Biomolecular Chemistry*
Manuscript ID	OB-ART-08-2024-001350.R1
Article Type:	Paper
Date Submitted by the Author:	31-Oct-2024

Complete List of Authors:

Seio, Kohji; Tokyo Institute of Technology, Department of Life Science and Technology
Ohnishi, Rie; Tokyo Institute of Technology, Department of Life Science and Technology
Tachibana, Shigetoshi; Tokyo Institute of Technology, Department of Life Science and Technology
Mikagi, Hiroki; Tokyo Institute of Technology, Department of Life Science and Technology
Masaki, Yoshiaki; Tokyo Institute of Technology, Department of Life Science and Technology

ARTICLE

Synthesis of LNA gapmers that replace a phosphorothioate linkage with a sulfonamide in the gap region, and their ability to form duplexes with complementary RNA targets

Received 00th January 20xx,
Accepted 00th January 20xx

DOI: 10.1039/x0xx00000x

Kohji Seio,* Rie Ohnishi, Shigetoshi Tachibana Hiroki Mikagi, and Yoshiaki Masaki*

Antisense oligodeoxynucleotides can bind to target RNAs and cleave them using RNase H. Despite the high activity of antisense oligodeoxynucleitides modified with locked nucleic acids (LNA9 at several bases at both the 5' and 3' ends (LNA gapmer)), toxicity has been reported, necessitating additional backbone modifications to reduce toxicity. In this study, we introduced a sulfonamide linkage to the LNA gapmer to elucidate its fundamental properties such as hybridization, base recognition, and induction of RNase H activity. A new chemically stable sulfonyltriazole was used as a synthetic intermediate to introduce a sulfonamide linkage between the two nucleosides. We studied the properties of the duplex of the sulfonamide-linked gapmer and target RNAs, such as melting temperature, circular dichroism, and cleavage of RNA strands by RNase H. We found that the gapmers had a lower but tolerable duplex stability with base-pair specificity and the ability to induce RNase H activity.

Introduction

Antisense oligonucleotides (ASOs) are single−stranded artificial oligonucleotides that bind to complementary RNAs in the cell and inhibit their translation.[1] When an ASO contains consecutive deoxynucleotide residues, the duplex of the ASO and target RNA is recognized by RNase H, and the RNA is cleaved. ASOs that inhibit the translation of target RNAs via this RNase H-dependent mechanism have been extensively studied. To improve the properties of ASOs, a molecular design called a "gapmer" is used, in which some deoxynucleotide residues of both termini in the wing-regions are replaced with 2'-O-modified ribonucleotide residues such as 2'-O-methoxyethyl (MOE)-nucleotides.[2] Some clinically approved ASOs such as mipomersen,[3] inotersen,[4] and volanesorsen[5] are categorized as this type.

For gapmers, the chemical modification of oligonucleotides is essential to increase the stability of ASOs in serum and improve their binding affinity to target RNAs. For this purpose, phosphorothioate[6] and other backbone modifications[7] and 2'-modifications[8,9] including bridged nucleic acids[10,11,12] have been studied.

Recently, the purpose of chemical modifications has shifted from improving enzymatic stability and RNA affinity to enhancing safety and improving the therapeutic index. For example, the introduction of a 2'-modification,[13] 5'-C-modification,[14] or base modification[15] into the gap region of the gapmer has been reported to ameliorate the cytotoxicity or hepatotoxicity of some toxic gapmers. In addition, it has been reported that modification of the internucleotide linkage to a mesylphosphoroamidate[16] or alkylphosphonate[17] is effective. These results suggest the usefulness of the modification of the phosphate backbone; however, the modification of phosphorus generates diastereomers, which should be stereochemically controlled[7,18,19] or carefully analyzed[20] to control the quality of therapeutic ASOs when they are synthesized in a stereo-random manner.

Sulfonamide-linked oligonucleotides,[21,22] which are nucleic acid analogs with achiral internucleotidic linkages, have been synthesized and studied (Figure 1). Sulfonamides are considered similar to phosphates because they typically contain a third-period element (P or S) flanked by two second-period atoms (O, C, or N). In addition, they contain P=O or S=O bonds with large dipole moments. Several sulfonamide-linked oligodeoxynucleotides were synthesized, and their fundamental properties were investigated. As a result, oligodeoxynucleotides incorporating sulfonamide-1 (Figure 1) formed duplexes with complementary DNA, lowering the melting temperature (T_m) by 3-4 °C/modification.[21] Similarly, the incorporation of sulfonamide-2 (Figure 1) resulted in a T_m decrease of 4 °C/modification for the duplex with complementary RNA.[22]

Despite these synthetic and physicochemical studies, the properties of sulfonamide linkages in gapmers have not yet been reported. As described above, a recent study clarified that the site-specific modification of gapmers has profound effects on their therapeutic indices. In addition, we also reported that single-point modification of the internucleotide linkage altered the interaction between a gapmer and RNase H, allowing allele-specific cleavage of the target RNA.[23] Thus, the use of

[a] *Department of Life Science and Technology, Tokyo Institute of Technology, 4259 Nagatsuta-cho Midori-ku, 226-8501, Yokohama, Japan*

† Footnotes relating to the title and/or authors should appear here.

Electronic Supplementary Information (ESI) available: [details of any supplementary information available should be included here]. See DOI: 10.1039/x0xx00000x

sulfonamide may outweigh the disadvantages of a lower T_m. In addition, the incorporation of locked nucleic acids into the wing region, which increases the affinity for the target RNA, may compensate for the lowered T_m. Based on these considerations, we synthesized two gapmers incorporating a structure sulfonamide-1 and investigated their basic properties such as affinity to target RNA, ability to recognize the counter base, and ability to induce cleavage of target RNA by RNase H, which are essential properties for ASOs.

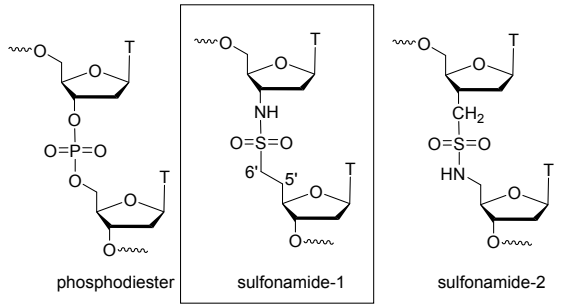

Figure 1. Chemical structures of dimer units containing phosphodiester or sulfonamide linkages.

Results and discussion

Synthesis of the phosphoramidite of sulfonamide-linked nucleoside dimers and oligonucleotides

The synthesis of oligonucleotides containing a sulfonamide linkage was reported previously.[21] We followed this procedure with slight modifications using a new sulfonylating intermediate **4**. Thymidine unit **4** was synthesized from tetra(*n*-butyl)ammonium compound **1**. [24] The cation was changed to a sodium cation by passing it through a cation-exchange resin to give **2**. To convert sulfonate **2** into chloride **3**, cyanuric chloride[25] was used in the presence of 18-crown-6 and chloride **3** was successfully obtained as an intermediate. In addition, intermediate **3** reacted with 1,2,4-triazole to give the new **4** in 92% yield from **2**. Because of the stability of sulfonyltriazole, as reported previously,[25b] compound **4** was stable during purification by silica gel column chromatography and could be stored stably. Using **4**, the dimer **6** was synthesized by reaction with 3'-deoxy-3'-amino-5'-(4-methoxytrityl)thymidine **5** (Scheme 1).[26,16] The dimer **6** was converted to the phosphoramidite **8** by the usual deprotection of the TBDMS group to give **7**, and subsequent phosphitylation by reaction with 2-cyanoethyl *N*,*N*-diisopropylchlorophosphoramidite in the presence of *N*,*N*-diisopropylethylamine.

The sulfonyltriazole derivative **4** was also used to synthesize dimer **10**. Compound **4** was reacted with 3'-deoxy-3'-amino-6-*N*-benzoyl-5'-(4, 4'-dimethoxytrityl)deoxyadenosine **9**[27] to give dimer **10,** which was converted to the 3'-hydroxy derivative **11** in 68% yield in the 2-step reaction. The coupling of **4** and **9** was carried out at room temperature for 9 days to minimize the side reaction of acyl transfer from the base moiety to the 3'-amino group. Compound **11** was also converted to phosphoramidite **12**. Phosphoroamidites **8** and **12** were used for oligonucleotide synthesis after the removal of reagent residues using flush column chromatography.

We synthesized two phosphorothioate gapmers whose sequences were **ON1**: 5'-CCAd(GTTnscTCCGCAT)GAT-3' and **ON2**: 5'-TCGd(GAAnscTCATAGT)AGT-3', in which the underlined residues are LNA,[11] and 'nsc' indicates the sulfonamide linkage. The oligonucleotides were synthesized as follows: First the 3'-half of the oligonucleotides just before the sulfonamide dimer was synthesized on solid supports using a DNA synthesizer. The sulfonamide dimers were manually introduced into these oligonucleotides as described in the Experimental section. The 5'-half of the oligonucleotide following the sulfonamide dimer was then extended using a DNA synthesizer. The deprotection and cleavage of the solid supports were performed using aqueous ammonia. The products were purified by reversed-phase HPLC, and their structures were confirmed by MALDI-TOF mass spectrometry. As controls, we purchased **ON3** and **ON4,** which are phosphorothioate oligonucleotides with the same sequences and LNA wings as **ON1** and **ON2**, respectively. The sequences of **ON1–ON4** are shown in Figure 2, along with the RNA strands used in the subsequent experiments.

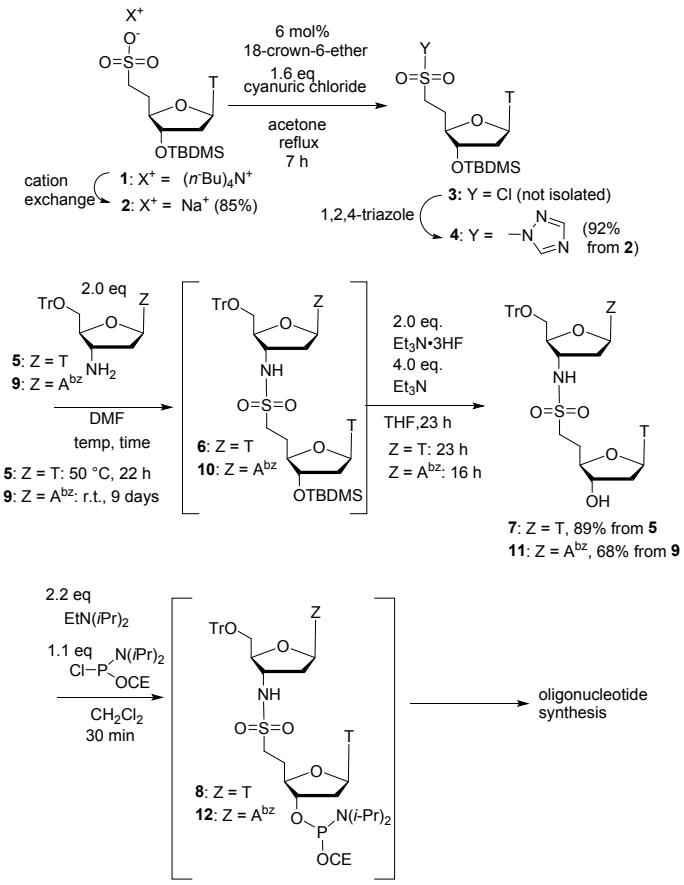

Scheme 1. Synthesis of the sulfonyltriazole derivative **4** and the phosphoramidite of sulfonamide-linked thymidine dimer **8**. Tr=MMTr for Z = T, and DMTr for Z = A^{bz}。 CE=2-cyanoethyl group

ON1: 5'-CCA d(GTTnscTCCGCAT) GAT-3'
ON2: 5´-TCG d(GAAnscTCATAGT) AGT-3´
ON3: 5'-CCA d(GTTTCCGCAT) GAT-3'
ON4: 5´-TCG d(GAATCATAGT) AGT-3´

RNA1a: 3'-GGUCAaaGGCGUACUA-5'
RNA1b: 3'-GGUCAcaGGCGUACUA-5'
RNA1c: 3'-GGUCAacGGCGUACUA-5'
RNA1d: 3'-GGUCAaaGGCGUACUA-FAM-5'

RNA2a: 3'-AGCCUuaGUAUCAUCA-5'
RNA2b: 3'-AGCCUcaGUAUCAUCA-5'
RNA2c: 3'-AGCCUucGUAUCAUCA-5'
RNA2d: 3'-AGCCUuaGUAUCAUCA-FAM-5'

Figure 2. The sequences of oligonucleotides used in this study. Underlines indicate that the residues are LNA, and 'nsc' indicates the sulfonamide linkage. **RNA1a** and **RNA2a** are the complementary sequences to **ON1** and **ON2**, respectively. **RNA1b**, **c** and **RNA2b**, **c** are single base mismatched sequences for **ON1** and **ON2**, respectively. **RNA1d** and **RNA2d** are FAM-labelled derivatives of **RNA1a** and **RNA2a**, respectively. In **RNA1a**-**d**, and **RNA2a**-**d**, the lowercases indicate that these residues face sulfonamide dimer units TnscT or AnscT.

Hybridization properties and circular dichroism of the oligonucleotides.

Table 1. Melting temperatures (°C), of the duplexes. Values in parentheses indicate the differences from the duplexes with **RNA1a** of **RNA2a**. The thermodynamic parameters for the formation of full-matched duplexes were also shown.

	RNA1a	**RNA1b**	**RNA1c**
ON1	67.1±0.3	58.5±0.2 (-8.6)	58.1±0.04 (-9.0)
ON3	69.7±0.4	59.3±0.1 (-10.4)	58.9±0.1 (-10.8)
	RNA2a	**RNA2b**	**RNA2c**
ON2	57.8±0.6	49.9±0.1 (-7.9)	48.3±0.1 (-9.5)
ON4	60.8±0.3	53.0±0.2 (-7.8)	50.8±0.1 (-10.0)

Table 2. Thermodynamic parameters for full-matched duplexes

	ΔH (kcal mol^{-1})	ΔS (cal mol^{-1} K^{-1})	ΔG_{37} (kcal mol^{-1})
ON1/RNA1a	-126±5	-343±15	-19±0.4
ON3/RNA1a	-123±4	-334±12	-20±0.4
ON2/RNA2a	-110±4	-306±12	-15±0.3
ON4/RNA2a	-122±6	-341±17	-17±0.4

The melting temperatures (T_ms) of the duplexes of **ON1** to **ON4** with the complementary RNA strands **RNA1a** and **RNA2a** were measured (Figure 1) and are summarized in Table 1. **RNA1a** is the complementary sequence of **ON1** and **ON3**. **RNA2a** is complementary to **ON2** and **ON4**. UV melting curves shown in the Supporting Information show the two-state transitions that resulted in T_m values of 67.1±0.3, 69.7±0.4, 57.8±0.6, 60.8±0.3 °C for **ON1**/**RNA1a**, **ON3**/**RNA1a**, **ON2**/**RNA2a**, and **ON4**/**RNA2a**, respectively. The comparison of **ON1**/**RNA1a** and **ON3**/**RNA1a** revealed that the incorporation of a sulfonamide linkage into the LNA-DNA-LNA gapmer reduced the T_m by 2.6 °C. Similarly, when comparing **ON2**/**RNA2a**, and **ON4**/**RNA2a**, the sulfonamide linker reduced the T_m by 3.0 °C. These values were comparable to previous reports of DNA-DNA duplexes.[21,22] Although the T_m values of the gapmers were lowered by 3.0 °C by the incorporation of the sulfonamide linkage, this does not necessarily indicate the loss of ASO activity. For example, the T_m of **ON1**/**RNA1a**, which was 67 °C, is within the range 62-76 °C reported in a study[28] that is necessary for high ASO activity. Although the T_m of **ON2**/**RNA2a** was too low according to these criteria, this was not solely due to the incorporation of the sulfonamide linker, but also due to the intrinsically low T_m of **ON4**/**ON2a**. In addition to the T_m values, the thermodynamic parameters of duplex formation were derived as shown in Table 2. It should be noted that the thermodynamic parameters here represent approximate values for the mixture and do not reflect those of pure materials, as **ON1** to **ON4** are mixtures of diastereomers of internucleotidic phosphorothioates. Interestingly, the less stable **ON1**/**RNA1a** duplex showed a more negative ΔH, and a less negative ΔS in comparison with **ON3**/**RNA1a** duplex. This suggests that **ON1**/**RNA1a** duplex was entropically destabilized. In comparison, for **ON2**/**RNA2a**, and **ON4**/**RNA2a**, ΔH and ΔS of **ON2**/**RNA2a** were less negative and more negative, respectively, than those of **ON4**/**RNA2a**, that suggested that **ON2**/**RNA2a** was destabilized enthalpically. The possible mechanisms for these differences are discussed in the next section.

In addition to the stability of sequence-matched duplexes, we also investigated the stability of duplexes containing one mismatched base pair. We used **RNA1b** and **1c** for **ON1** and **RNA2b** and **2c** for **ON2**. **RNA1b** and **RNA1c** were designed to form a TC mismatch base pair with the 5'-side or 3'-side thymine in the sulfonamide dimer unit of **ON1**. **RNA2b** and **RNA2c** were designed to form AC and TC mismatched base pairs with the 5'-side adenine or 3'-side thymine, respectively, in the sulfonamide dimer unit of **ON2**. Here, we chose AC and TC mismatches as standards for unpaired bases because, unlike A-G or T-G pairs, they do not form stable base pairs. In the case of **ON1**, the T_m values with **RNA1b** and **RNA1c** were 58.5 and 58.1 °C, respectively. The decrease in T_m from the sequence-matched **ON1**/**RNA1a** was 8.6 and 9.0 °C, respectively. To compare the T_m decreases with that of **ON3**, we also measured the T_m of the **ON3**/**RNA1b** and **ON3**/**RNA1c** duplexes, which were 59.3 and 58.9 °C, respectively, and the T_m decreases from the **ON3**/**RNA1a** duplex were 10.4 and 10.8 °C. Although these T_m decreases were reduced by the introduction of the sulfonamide linkage, the higher T_m of **ON1**/**RNA1a** compared to **ON1**/**RNA1b** and **ON1**/**RNA1c** suggests that the two thymine residues of the sulfonamide dimer unit in **ON1** recognized the bases at the opposite position of the RNA strand, forming Watson-Crick base pairs. We also measured the T_ms of the duplexes of **ON2** or **ON4** with **RNA2b** and **RNA2c**. The T_ms of **ON2**/**RNA2b**, **ON2**/**RNA2c**, **ON4**/**RNA2b**, and **ON4**/**RNA2c** were 49.9, 48.3, 53.0, and 50.8 °C, respectively. The decrease in T_m due to the 5'- and 3'-side mismatches were 7.9 and 9.5 °C for **ON2**, and 7.8 and 10.0 °C for **ON4**, respectively. These data suggest that the 5'- and 3'-side nucleobases of the sulfonamide dimer unit in **ON2** also recognized the bases at the opposite position.

Conformation of the oligonucleotides and dimer incorporating the sulfonamide linkage

To gain insight into the conformation of the gapmers incorporating the sulfonamide linkage, we measured the CD spectra of **ON1**/**RNA1a**, **ON3**/**RNA1a**, **ON2**/**RNA2a**, and **ON4**/**RNA2a** (Fig. 3). All CD spectra showed a negative band at approximately 240 nm and a large positive band at 260 nm, typical of an A-type duplex. No change was observed between the CD spectra of the duplexes incorporating sulfonamides, such as **ON1**/**RNA1a** and **ON2**/**RNA2a**, and the parent **ON3**/**RNA1a** and **ON4**/**RNA2a**.

Since the T_m experiments showed that the nucleobases in the sulfonamide dimer units in **ON1** and **ON2** recognized the nucleobase at the opposite position, it is expected that the sulfonamide dimer unit fits the canonical A-type structures in the ASO-RNA duplexes, forming Watson-Crick base pairs. Additionally, the decrease in T_m upon incorporation of the sulfonamide linkage was likely not due to distortion of the duplex structure.

Therefore, we also measured the CD spectra of the fully deprotected dimers TnscT (**13**) and AnscT (**14**), prepared by the deprotection of **7** and **11**, respectively, at different temperatures (Figure 4). The CD spectra of **13** and **14** were compared with thymidyl(3', 5')thymidine (TpT), and deoxyadenosyl(3', 5')thymidine (ApT). As shown in Figure 4, both TpT (Figure 4A) and ApT (Figure 4C) exhibited a negative band at approximately 250 nm, and a positive band at approximately 280 nm, both of which decreased as the temperature increased from 10 to 60 °C. This temperature-dependent change was due to the conformational change of TpT and ApT from the base-stacked to the base-unstacked random-coil conformation. In contrast, in the cases of **13** (Figure 4B) and **14** (Figure 4D), the CD signals at 10 °C were as small as those of TpT and ApT at 60 °C. These signals exhibited only slight changes with increasing temperature. These results showed that **13** and **14** did not adopt the natural base-stacked conformation, even at 10 °C. This indicated that the conformation corresponding to the A-type structure, which adopts a base-stacked conformation, was not the preferred conformation for the sulfonamide dimer unit. The instability of the base-stacked conformation of the sulfonamide dimer unit was expected to lead to a decrease in the T_ms of the duplexes. Moreover, the peak around 280 nm of 14 blue-shifted by 3 nm at 0 °C, as shown in Figure 4D. This suggests that the conformation of 14 at low temperatures differs from both the random-coil and naturally stacked forms. In contrast, 13, which showed neither a blue- nor red-shift, is expected to adopt a random-coil conformation even at low temperatures. Such conformational properties may account for the thermodynamic parameters shown in Table 2. As discussed in the previous section, **ON1**/**RNA1a** was entropically destabilized. This may be due to the flexibility of dimer unit **13** in **ON1**, which leads to a loss of entropy upon duplex formation. Conversely, if the dimer unit **14** in **ON2** forms a stable conformation, as suggested by Figure 4D, the conformational change upon duplex formation may lead to enthalpic destabilization.

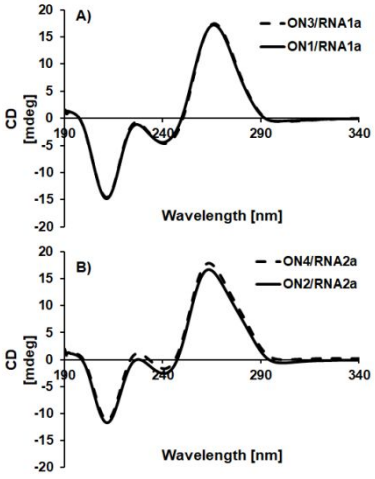

Figure 3. CD spectra of A) **ON1**/**RNA1a** and **ON3**/**RNA1a**, and B) **ON2**/**RNA2a** and **ON4**/**RNA2a**.

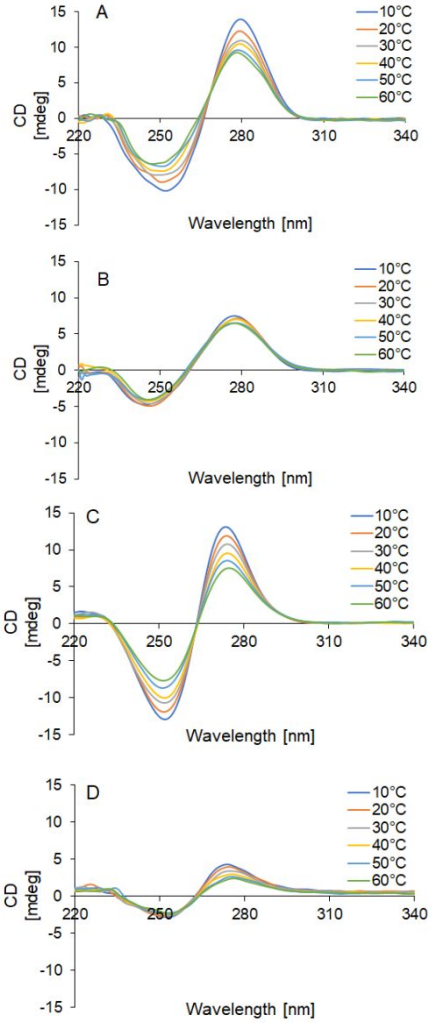

Figure 4. CD spectra of the dimer units. A) TpT, B) TnscT (**13**), C) dApT, and D) dAnscT (**14**)

Induction of RNase H activity by gapmers introducing a sulfonamide linkage.

As described above, the LNA-DNA-LNA gapmers introduce a sulfonamide linkage and recognize complementary RNAs. Thus, when the RNA strands in the gapmer-RNA duplexes are cleaved by RNase H, gapmers incorporating a sulfonamide linkage are expected to be useful as ASOs. Therefore, we investigated the cleavage of RNA strands hybridized to gapmers **ON1** and **ON3** by RNase H. We mixed **ON1** or **ON2** with FAM-labelled complementary **RNA1d** and **RNA2d** (Figure 2) and *E. coli* RNase H. The products were analyzed using polyacrylamide gel electrophoresis (Figure 5). These reactions were compared to those of **ON3** and **ON4**.

As shown in Figure 5A, in the presence of **ON3**, **RNA1d** was cleaved, with less than 10% of the full-length RNA remaining within 5 min. When **ON1** was used instead of **ON3**, RNA was also cleaved. However, the rate of cleavage was slower than that with **ON3,** taking 15 min to cleave 90% of **RNA1d**. Similar experiments were performed with **ON2**, **ON4,** and **RNA2d**, which showed similar time courses (Figure 5B). These results clearly demonstrate that LNA-DNA-LNA gapmers containing a sulfonamide linkage are capable of inducing the cleavage of hybridized RNA by RNase H. As shown in Figure 5A, cleavage induced by **ON1** occurred at sites that yielded the 9-, 10-, and 11-mer products. As shown in Figure 6, the 9-mer and 11-mer were generated by cleavage at the 5'-upstream and 3'-downstream positions of the two consecutive adenosines, shown by 'aa' in Figure 6, facing the TnscT unit. The 10-mer was generated by cleavage of the phosphodiester bond at the opposite position to the sulfonamide linkage. These results clearly indicated that the incorporation of a sulfonamide linkage did not prevent the cleavage of the bound RNA near or opposite to the sulfonamide linkage. In the case of **ON2**, cleavage produced 8-mer, 9-mer, and 10-mer fragments, suggesting cleavage near the sulfonamide linkage, as shown in Figure 6.

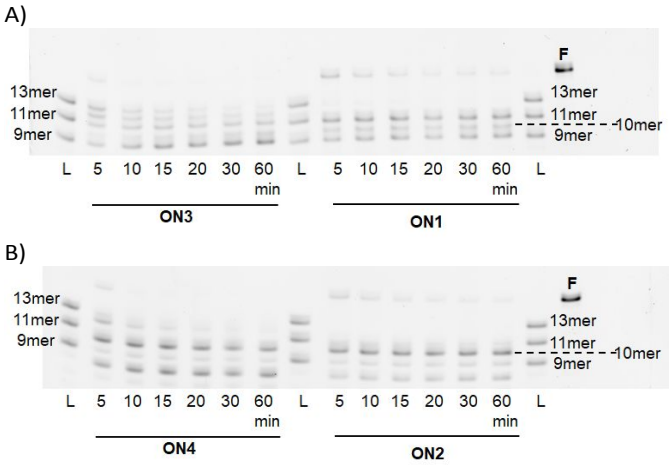

Figure 5. Cleavage of FAM-labelled RNA with RNase H in the presence of the LNA-DNA-LNA gapmer. A) Cleavage of **RNA1d** in the presence of **ON1** or **ON3**. B) Cleavage of **RNA2d** in the presence of **ON2** or **ON4**. The materials in the ladder's lanes are: in panel A) 13-mer: 3'-CAaaGGCGUACUA-FAM-5', 11-mer: 3'-aaGGCGUACUA-FAM-5', and 9-mer: 3'-GGCGUACUA-FAM, and in panel B) 13-mer: 3'-CUuaGUAUCAUCA-FAM-5', 11-mer: 3'-uaGUAUCAUCA-FAM-5', and 9-mer: 3'-GUAUCAUCA-FAM-5', which were loaded as the size markers. **F** represents **RNA1d** or **RNA2d**.

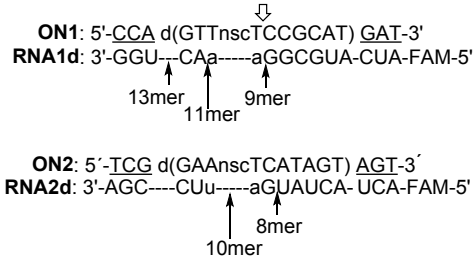

Figure 6. Cleavage sites of **RNA1d** and **RNA2d**. The arrows indicate the positions of phosphodiester bonds which were cleaved to give the indicated products. The lowercase indicates that the bases formed base pairs with the bases in the sulfonamide dimer units. The blank arrow indicates the phosphate which is recognized by the phosphate-binding pocket of RNaseH when the 11-mer product was formed (see discussion in the Conclusions section).

Conclusions

In this paper, we reported the synthesis and properties of LNA-DNA-LNA gapmers with sulfonamide linkages. First, we evaluated the usefulness of sulfonyltriazole **4** as a synthetic intermediate for introducing the sulfonamide linkage. We previously reported the use of another sulfonyltriazol derivative for the synthesis of 2'-O-sulfamoylpropylnucleoside.[25b] Thus, the protocol for activating sulfate to sulfonyltriazole is useful for the synthesis of various sulfonamide-modified nucleoside derivatives. An important finding of this study is that the gapmer incorporating a sulfonamide linkage can retain properties that are important for ASOs. These properties include the binding affinity to complementary RNAs, discrimination of mismatched targets, and induction of RNase H-dependent target RNA cleavage. In terms of binding affinity, although the T_m decreased by approximately 3 °C upon the introduction of the sulfonamide linker, this was expected to be small enough to maintain the knockdown activity of the parent gapmer, if it was designed to have high affinity towards the target RNA. However, if the affinity of the parent gapmer is low, the introduction of sulfonamide may cause the knockdown activity to be lost.

The CD spectra of the dimer units (Figure 4) show that the sulfonamide-linked dimers did not adopt a base-stacked conformation. This is probably because the C4'-C5' bond did not adopt the *g+* conformation due to the steric clash between the methylene attached to the 5'-CH_2 and the base or sugar moiety. The sulfamate oligonucleotide, which were linked through 5'O-SO_2-N3' linkages, was reported as an nucleic acid analog which contained a sulfonamide and formed a more stable duplex with the opposite strand.[29,30,31,] However, its usefulness in therapeutic gapmers is still to be determined when the thermal instability of the sulfamoyl structure[32] is considered. Another potential method to improve the affinity of sulfonamide-linked oligonucleotides may be to modulate the C4'-C5' conformation by introducing a 5'-methyl group or other substituent.[14]

Regarding the induction of RNA cleavage by RNase H, our results are rationalized by the three-dimensional structure of the DNA-RNA-RNase H complex[33], which suggests that the phosphate-binding pocket recognizes the phosphate of a 5'-deoxynucleotide residue and cleaves the phosphate of the 5'-

ribonucleotide residue that base-pairs with the deoxynucleotide residue located at the third 5′-upstream position from the 5′-deoxynucleotide residue captured by the phosphate binding pocket (Figure 6, empty arrow for the production of 11-mer). Thus, for all products shown in Figure 6, the sulfonamide bond was not involved in molecular recognition between RNase H and the gapmer-RNA duplex. In this study, we introduced the sulfonamide bond in the 5′-side of the gap region, because site-specific modification of these positions are reported to ameliorate the toxicity of gapmers.[13,16,17] The toxicity of the LNA-gapmer including sulfonamide backbone should be experimentally clarified. Therefore, interactions of the sulfonamide group and RNase H should be studied separately when sulfonamide modifications are introduced to positions in the 3′-side of the gap.

Experimental

3′-*O*-(*t*-Butyldimethylsilyl)-5′-deoxy-5′-sulfomethylthymidine sodium salt (2). Compound **1** (ref) (5.28 g, 7.84 mmol) was dissolved in H_2O-CH_3OH (1:1, v/v) and applied to the column filled with a cation exchange resin Na^+ form (DOWEX™ 50w×8, 200-400 mesh, 30 g). The material was eluted by washing with H_2O-CH_3OH (1:1, v/v) and the fraction was concentrated. The residue was then purified by flash column chromatography on silica gel (60N, 100 g). The material was eluted with CH_2Cl_2-CH_3OH (98:2, v/v to 80:20, v/v) to give **2** (3.19 g, 85%). ^{1}H NMR (400 MHz, DMSO-d_6) δ 11.31 (s, 1H), 7.42 (s, 1H), 6.10 (t, J = 7.0 Hz, 1H), 4.24-4.21 (m, 1H), 3.70-3.67 (m, 1H), 2.55-2.39 (m, 2H), 2.26-2.19 (m, 1H), 2.03-2.01 (m, 1H), 2.00-1.97 (m, 1H), 1.94-1.89 (m, 1H), 1.80 (s, 3H), 0.87 (s, 9H), 0.080 (m, 6H); ^{13}C NMR (101 MHz, DMSO-d_6) δ 163.75, 150.47, 136.08, 109.98, 85.11, 83.31, 74.60, 47.98, 40.19, 29.29, 25.74, 17.70, 12.15, -4.67, -4.80; ESI-TOF mass: calcd for $C_{17}H_{29}N_2O_7SSi$- [M–Na]]$^-$ 433.1470, found 433.1467.

3′-*O*-(*t*-Butyldimethylsilyl)-5′-deoxy-5′-triazolylsulfonylmethylthymidine (4). Compound **2** (750 mg, 1.64 mmol) was co-evaporated three times each with anhydrous pyridine and anhydrous toluene, and then dissolved in anhydrous acetone (16.4 mL). To the solution was added 18-crown-6-ether (25.4 mg, 0.096 mmol) and cyanuric acid chloride (490 mg, 2.66 mmol). The reaction was stirred at 68 °C for 7 h under argon. Then, 1,2,4-triazole (2.30 g, 33.0 mmol) was added. The reaction mixture was stirred at 68 °C for 10 h under argon. The system was cooled to ambient temperature, and then filtered on celite. The solution was concentrated, diluted with CH_2Cl_2 (150 mL), washed with saturated aqueous $NaHCO_3$ (75 mL) three times, and saturated aqueous NaCl (75 mL) three times. The organic layer was dried over Na_2SO_4, filtered and concentrated under reduced pressure. The residue was purified by flash column chromatography on silica gel (60N, 25 g). The material was eluted with *n*-hexane-ethyl acetate (9:1, v/v to 4:6, v/v) to give **4** (731 mg, 92%). ^{1}H NMR (400 MHz, $CDCl_3$) δ 8.69 (s, 1H), 8.15 (s, 1H), 7.98 (s, 1H), 6.96 (s, 1H), 6.03 (t, J = 6.7 Hz, 1H), 4.16-4.11 (m, 1H), 3.81-3.72 (m, 2H), 3.68-3.60 (m, 1H), 2.32-2.22 (m, 2H), 2.21-2.12 (m, 1H), 2.08-1.98 (m, 1H), 1.96 (s, 3H), 0.87 (s, 9H), 0.07 (s, 6H) ; ^{13}C NMR (101 MHz, $CDCl_3$) δ 163.07, 154.55, 149.72, 145.24, 136.02, 111.62, 86.16, 83.29, 74.70, 51.41, 39.72, 26.69, 25.72, 17.97, 12.68, -4.48, -4.77 ; ESI-TOF mass : calcd for $C_{19}H_{31}N_5O_6SSi$ [M+Na]$^+$ 508.1657, found 508.1664.

Thymidine dimer linked via sulfonamide linkage (7) Compound **4** (487 mg, 1.00 mmol) was dissolved in anhydrous dimethylformamide (1 mL). 3′-Amino-5′-(4-monomethoxytrityl)-3′-deoxythymidine (**5**, 1.03 g, 2.00 mmol) was then added. The reaction was stirred at 50 °C for 22 h under argon. The reaction mixture was diluted with ethyl acetate (100 mL) and washed three times with H_2O (50 mL). The organic layer was dried over Na_2SO_4, filtered and concentrated under reduced pressure. The residue was purified by flash column chromatography on silica gel (60N, 25 g). The elution was performed with *n*-hexane-ethyl acetate (8:2, v/v to 2:8, v/v) to give **6** (743 mg, 0.80 mmol). This compound was dissolved in anhydrous tetrahydrofuran (8.0 mL). Triethylamine (446 µL, 3.2 mmol) and triethylamine trihydrofluoride (261 µL, 1.6 mmol) were then added. The reaction mixture was stirred under argon for 23 h under at room temperature. Next, trimethylethoxysilane (3.8 mL, 24 mmol) was added and the reaction mixture was stirred at room temperature for 16 h under argon and then concentrated. The residue was purified by flash column chromatography on silica gel (60N, 20 g). The elution was performed with CH_2Cl_2-CH_3OH (98:2, v/v to 92:8, v/v) to give **7** (580 mg, 89%). ^{1}H NMR (400 MHz, CD_3CN) δ 8.98 (br, 2H), 7.47-7.44 (m, 5H), 7.33-7.29 (m, 6H), 7.27-7.23 (m, 2H), 7.18-7.17 (m, 1H), 6.89-6.85 (m, 2H), 6.19-6.16 (dd, *J* = 7.2 Hz, 5.2 Hz, 1H), 6.12-6.09 (t, *J* = 6.8 Hz, 1H), 5.71-5.68 (br, 1H), 4.28-4.20 (m, 1H), 4.16-4.11 (m, 1H), 3.94-3.91 (m, 1H), 3.76 (s, 3H), 3.73-3.68 (m, 1H), 3.44-3.43 (br, 1H), 3.39-3.36 (m, 1H), 3.32-3.28 (m, 1H), 3.14-3.02 (m, 2H), 2.52-2.45 (m, 1H), 2.38-2.31 (m, 1H), 2.24-2.19 (m, 2H), 2.13-2.12 (m, 2H), 1.80 (d, 3H), 1.50 (d, 3H) ; ^{13}C NMR (101MHz, CD_3CN) δ 164.53, 164.48, 159.85, 151.30, 145.35, 145.32, 137.02, 136.68, 136.05, 131.40, 129.27, 128.94, 128.14, 114.10, 111.51, 111.24, 87.65, 85.34, 84.96, 84.64, 84.35, 74.37, 63.29, 55.90, 53.42, 50.34, 39.51, 39.24, 28.25, 12.47, 12.32 ; ESI-TOF mass : calcd for $C_{41}H_{45}N_5O_{11}S$ [M+Na]$^+$ 838.2728, found 838.2734.

Compound 11. Compound **4** (327 mg, 0.67 mmol) was dissolved in anhydrous dimethylformamide (1 mL). 3′-amino-6-N-benzoyl-5′-(4-monomethoxytrityl)-2′,3′-dideoxyadenosine (**9**, 859 mg, 1.31 mmol) was then added. The reaction mixture was stirred at room temperature for 9 days under argon. The reaction mixture was diluted with ethyl acetate (100 mL) and washed with H_2O (50 mL) for three times. The organic layer was dried over Na_2SO_4, filtered and concentrated under reduced pressure. The residue was purified by flash column chromatography on silica gel (60N, 15 g). The elution was performed with *n*-hexane-ethyl acetate (7:3, v/v to 0:10, v/v) to yield **10** (483 mg, 0.45 mmol). This compound was dissolved in anhydrous tetrahydrofuran (4.5 mL). Triethylamine (251 µL, 1.8 mmol) and triethylamine trifluoride (147 µL, 0.90 mmol) were then added. The reaction was stirred at room temperature for 16 h under argon. Next, trimethylethoxysilane (2.1 mL, 13.5 mmol) were added and the reaction stirred at room temperature for 16 h under argon and then concentrated. The residue was purified by flash column chromatography on silica gel (60N, 10 g). The elution was performed with CH_2Cl_2-CH_3OH (100:0,

v/v to 95:5, v/v) to yield **11** (292 mg, 68%). ^{1}H NMR (400 MHz, CD_3CN) δ 9.33 (br, 1H), 9.06 (br, 1H), 8.64 (s, 1H), 8.30 (s, 1H), 8.00 (d, 2H), 7.65 (m, 1H), 7.55 (m, 1H), 7.33-7.30 (m, 2H), 7.22-7.16 (m, 8H), 6.77-6.73 (m, 4H), 6.43-6.40 (dd, *J* = 7.4 Hz, 3.4 Hz, 1H), 6.10 (t, *J* = 6.8 Hz, 1H), 5.74-5.71 (br, 1H), 4.66-4.58 (m, 1H), 4.15-4.10 (m, 1H), 4.05-4.01 (m, 1H), 3.72 (s, 6H), 3.71-3.67 (m, 1H), 3.46-3.45 (br, 1H), 3.40-3.36 (m, 1H), 3.24-3.21 (m, 1H), 3.17-3.14 (m, 2H), 2.64-2.56 (m, 1H), 2.24-2.19 (m, 2H), 2.13-2.09 (m, 3H), 1.78 (d, 3H) ; ^{13}C NMR (101 MHz, CD_3CN) δ 166.12, 164.58, 159.56, 159.54, 152.85, 152.64, 151.32, 150.79, 145.95, 143.83, 136.97, 136.83, 136.68, 134.79, 133.60, 130.96, 130.89, 129.67, 129.13, 128.91, 128.72, 127.76, 125.70, 113.90, 111.60, 87.02, 85.30, 84.98, 84.61, 74.41, 63.33, 55.83, 53.79, 50.18, 39.39, 38.31, 28.30, 12.47 ; ESI-TOF mass : calcd for $C_{49}H_{50}N_8O_{11}S$ $[M+Na]^+$ 981.3231, found 981.3214.

Synthesis of phosphoramidite 12. Compound **11** (214 mg, 0.22 mmol) was co-evaporated with anhydrous pyridine for seven times, toluene and CH_2Cl_2 for five times each, then dissolved in anhydrous CH_2Cl_2 (2.2 mL). To the solution were added *N, N*-diisopropylethylamine (83 µL, 0.49 mmol) and 2-cyanoethyl *N*, *N*-diisopropylchlorophosphoramidite (55 µL, 0.25 mmol). The reaction mixture was stirred at room temperature for 30 min under argon, diluted with CH_2Cl_2 (30 mL), washed with saturated aqueous $NaHCO_3$ (20 mL) for three times, and saturated aqueous NaCl (20 mL) once. The organic layer was dried over Na_2SO_4, filtered and concentrated under reduced pressure. The residue was purified by flash column chromatography on silica gel (60N, 5 g). The eluent was performed with *n*-hexane-ethyl acetate (1:1 to 0:10) to yield **12** (178 mg, 69%). ^{1}H NMR (400 MHz, CD_3CN) δ 9.31-9.22 (br, 1H), 9.03-8.97 (br, 1H), 8.64 (s, 1H), 8.30-8.29 (m, 1H), 8.01-7.99 (m, 2H), 7.68-7.63 (m, 1H), 7.57-7.53 (m, 2H), 7.34-7.32 (m, 2H), 7.22-7.16 (m, 8H), 6.77-6.73 (m, 4H), 6.43-6.40 (m, 1H), 6.10 (t, *J* = 7.0 Hz, 1H), 5.75-5.71 (m, 1H), 4.66-4.58 (m, 1H), 4.38-4.29 (m, 1H), 4.05-4.01 (m, 1H), 3.91-3.79 (m, 2H), 3.72 (s, 6H), 3.66-3.56 (m, 2H), 3.40-3.37 (m, 1H), 3.25-3.12 (m, 4H), 2.68-2.53 (m, 3H), 2.35-2.26 (m, 2H), 2.08-2.03 (m, 3H), 1.79-1.76 (m, 3H), 1.12-1.15 (m, 12H) ; ^{13}C NMR (101 MHz, CD_3CN) δ 164.58, 159.55, 151.27, 145.98, 143.76, 137.13, 137.07, 136.79, 136.67, 133.59, 130.94, 129.66, 129.15, 128.90, 128.72, 127.76, 125.73, 119.80, 119.66, 113.89, 111.67, 87.03, 85.63, 85.51, 84.95, 84.64, 83.91, 83.87, 83.54, 83.48, 63.28, 59.40, 59.35, 59.22, 59.16, 55.84, 53.75, 50.12, 44.09, 44.03, 43.97, 43.91, 38.34, 28.15, 24.93, 24.90, 24.86, 24.83, 24.80, 24.74, 21.06, 21.05, 20.99, 20.97, 12.43 ; ^{31}P NMR (162 MHz, CD_3CN) : δ 148.8-148.7 ; ESI-TOF mass : calcd for $C_{58}H_{67}N_{10}O_{12}PS$ $[M+Na]^+$ 1181.4290, found 1181.4314.

Oligonucleotide synthesis

ASO was synthesized in the DMTr-ON mode using an automated DNA synthesizer. Each LNA phosphoramidite unit, except LNA-5-methyl-CBz, and each DNA phosphoramidite unit were dissolved in dehydrated acetonitrile to reach 0.1 M solution. LNA-5-methyl-CBz was dissolved in acetonitrile/dehydrated dichloromethane (1:1, v/v) to reach 0.1 M solution. The solutions were applied to the automated DNA synthesizer. Glen UnySupport 1000 (1 µmol) was packed into an empty column, and the oligonucleotides were synthesized according to the general protocol. During the course of the synthesis, a manual synthesis method (described in the next section) was employed for the introduction of **8** and **12**. After the synthesis was completed the oligonucleotides were cleaved from the solid-supports and deprotection of the base moiety was carried out by treatment with 28% ammonia at 55 °C for 16 h. After ammonia was removed using a centrifugal evaporator, the material was applied to C-18 cartridge column. The failure sequences were washed with 15% acetonitrile in 0.1 M ammonium acetate, and the 5'-Trityl group was removed by aq. 2% trifluoroacetic acid. The target sequence was eluted by 30% aqueous acetonitrile. The fraction was concentrated by lyophilization, and further purified by reversed-phase HPLC. The structures were confirmed by MALDI-TOF-Mass spectrometry. **ON1**: **ON2**:

Manual synthesis. The introduction of **8** was performed by transferring the solid-supports carrying 5´- d(CCGCAT)GAT -3´ synthesized by the automatic synthesizer into a glass filter sealable by a three-way cock with an argon balloon (hereinafter referred to as the solid-phase cylinder). First, deprotection of the 5´-terminal MMTr group on the solid-phase carrier was carried out using a 1% trifluoroacetic acid/dichloromethane solution, washed with dichloromethane and acetonitrile, and dried under vacuum for 5 min. In the coupling reaction, 20 equivalents of **8** and 40 equivalents of 1*H*-tetrazole were added to the solid-phase cylinder and dissolved in 1 mL of dehydrated acetonitrile. The mixture was then shaken under argon atmosphere for 24 minutes and then washed with acetonitrile. Next, a solution of DDTT dissolved in dehydrated pyridine/dehydrated acetonitrile (3:2, v/v) to a concentration of 0.05 M was added as a sulfurizing agent, and the internucleotidic phosphorus atom was sulfated by shaking for 7 minutes. Finally, after washing with acetonitrile and dichloromethane, the column was dried under vacuum for 10 min until sufficiently dry, and the oligonucleotide-loaded solid phase carrier was loaded onto an empty column to continue automated synthesis.

The introduction of compound 2.4 was performed by transferring the solid-phase carrier loaded with 5´- d(CATAGT)AGT -3´ synthesized in an automated synthesizer into a solid-phase cylinder sealable by a three-way cock with an argon balloon. First, the 5´-terminal DMTr group on the solid-phase carrier was deprotected using a 1% trifluoroacetic acid/dichloromethane solution, washed with dichloromethane and acetonitrile, and dried under vacuum for 5 min. Compound 2.4 was then introduced by coupling reaction. In the coupling reaction, 20 equivalents of phosphoramidite unit powder and 40 equivalents of activator (1H-tetrazole) were added to the solid phase cylinder and dissolved in 250 µL of dehydrated acetonitrile. The mixture was then shaken as it was under argon atmosphere for 48 minutes and then washed with acetonitrile. Next, DDTT was dissolved in dehydrated pyridine/dehydrated acetonitrile (3:2, v/v) to a concentration of 0.05 M as a sulfurizing agent, and sulfurized by shaking for 7 minutes. Then, after washing with acetonitrile, a solution of DMAP dissolved in dehydrated pyridine/acetic anhydride (9:1, v/v) to 0.1 M was added and capped by shaking for 3 min. Finally, after washing with acetonitrile and dichloromethane, the column was dried under vacuum for 10 min until sufficiently dry, and the oligonucleotide-loaded solid phase carrier was loaded onto an empty column

Measurements of UV-melting temperatures.

Each ASO/RNA duplex was dissolved in phosphate buffer (10 mM sodium phosphate, 100 mM sodium chloride, 0.1 mM EDTA, pH 7.0) to a concentration of 2.0 μM as the duplex. The solution was heated at 95 °C for 3 minutes, and allowed to cooled to 25 °C. The absorbance was measured at 260 nm at every 0.5 °C increasing the temperature from 25 °C to 95 °C at +0.5 °C/min, and also decreasing from 95 °C to 25 °C at -0.5 °C/min. The absorbance was then plotted against temperature to make melting curves. After smoothing by Savitzky-Golay method, the curves were differentiated against temperature, and the T_m was calculated as the temperature which gave the maximum first derivatives.

Calculation of thermodynamic parameters. The thermodynamic parameters were calculated by fitting the measured UV-melting curves to theoretical curves. First, the fractional population of duplex (α) at each temperature were calculated using the upper and lower linear-baselines. Here, equilibrium constant (K), the total concentration of oligonucleotides (C_t = 4 μM), and the α were connected by the equation,

$$K = \frac{2\alpha}{C_t(1-\alpha)^2}$$

According to the thermodynamic theory,

$$K = \exp\left(-\frac{\Delta H - T\Delta S}{RT}\right)$$

The ΔH, and ΔS values which gave α which best matched the experimentally determined α were determined by non-linear least square fitting method.

Circular dichroism (CD) spectra of duplexes and dimers.

Each ASO/RNA duplex was dissolved in phosphate buffer (10 mM sodium phosphate, 100 mM sodium chloride, 0.1 mM EDTA, pH 7.0) to reach the final concentration of 4.0 μM. The duplexes were annealed by heating at 95 °C for 3 min and allowed to stand at room temperature for 1 hour. CD spectra were measured at 20 °C using a circular dichroism dispersometer. The measurement range was 360 nm-190 nm. The scanning speed was 100 nm/min and measurements were made in 10 integrations.

In the measurements of dimers, the dimers were dissolved in H_2O-DMSO (95:5, v/v). The concentration of the dimers was 120 μM. Then, CD spectra were measured using a circular dichroism dispersometer at varying temperatures of 10 °C, 20 °C, 30 °C, 40 °C, 50 °C, and 60 °C. The measurement range is 350 nm-190 nm. The scanning speed was 200 nm/min and measurements were made in 8 or 10 integrations.

Digestion by RNaseH

2 μL of each ASO adjusted to 10 μM and 1 μL of 20 μM **RNA1d** of **RNA2d** were mixed with 20 μL of 4× annealing buffer (200 mM Tris-HCl (pH 8.3), 300 mM KCl, and 0.5 mM EDTA) and 57 μL of milli-Q water (solution A). The solution was incubated on a heat block at 95 °C for 2 minutes, and then incubated at 37 °C. Separately, 10 μL of *E. Coli* RNase H (0.1 U/μL, maker), 50 μL of 4× reaction buffer provided by the supplier, and 140 μL of milli-Q water (solution B) were kept on ice for 5 minutes. The reaction was initiated by adding 20 μL of solution B to 80 μL of solution A, and the mixture were incubated at 37 °C. To evaluate the reaction rates, 10 μL aliquots were taken at 5, 10, 15, 20, 30, and 60 minutes, and quenched by mixing with 10 μL of electrophoresis buffer (10 M urea, 50 mM EDTA-2Na, and 0.1 wt% bromophenol blue), and cooling to -25 °C. The 4 μL of these aliquots were then charged on 40% polyacrylamide-7 M urea gel, and then electrophoresed at 60 W at 60 °C for 30 minutes. After the electrophoresis, the bands were visualized using a fluorescent laser scanner.

Conflicts of interest

There are no conflicts to declare.

Data availability

The data supporting this article have been included as part of the Supplementary Information.

Acknowledgements

This study was partly supported by This research was supported by Japan Agency for Medical Research and Development (AMED) under Grant Number JP21fk0210089, JP24fk0210147. This study was also supported by Japan Science and Technology Agency (JST) JPMJSF2313. We also thank Materials Analysis Division, Tokyo Institute of Technology for ESI-TOF, and MALDI-TOF analysis.

Notes and references

1 S. T. Crooke, X.-H. Liang, B. F. Baker and R. M. Crooke, Antisense technology: A review, *J. Biol. Chem.*, 2021, **296**, 100416.

2 S. Freier, The ups and downs of nucleic acid duplex stability: structure-stability studies on chemically-modified DNAduplexes, *Nucleic Acids Res.*, 1997, **25**, 4429–4443.

3 M. E. Visser, G. Wagener, B. F. Baker, R. S. Geary, J. M. Donovan, U. H. W. Beuers, A. J. Nederveen, J. Verheij, M. D. Trip, D. C. G. Basart, J. J. P. Kastelein and E. S. G. Stroes, Mipomersen, an apolipoprotein B synthesis inhibitor, lowers low-density lipoprotein cholesterol in high-risk statin-intolerant patients: a randomized, double-blind, placebo-controlled trial, *Eur. Heart J.*, 2012, **33**, 1142–1149.

4 M. D. Benson, M. Waddington-Cruz, J. L. Berk, M. Polydefkis, P. J. Dyck, A. K. Wang, V. Planté-Bordeneuve, F. A. Barroso, G. Merlini, L. Obici, M. Scheinberg, T. H. Brannagan, W. J. Litchy, C. Whelan, B. M. Drachman, D. Adams, S. B. Heitner, I. Conceição, H. H. Schmidt, G. Vita, J. M. Campistol, J. Gamez, P. D. Gorevic, E. Gane, A. M. Shah, S. D. Solomon, B. P. Monia, S. G. Hughes, T. J. Kwoh, B. W. McEvoy, S. W. Jung, B. F. Baker, E. J. Ackermann, M. A. Gertz and T. Coelho, Inotersen Treatment for Patients with Hereditary Transthyretin Amyloidosis, *New Engl. J. Med.*, 2018, **379**, 22–31.

5 M. J. Graham, R. G. Lee, T. A. Bell, W. Fu, A. E. Mullick, V. J. Alexander, W. Singleton, N. Viney, R. Geary, J. Su, B. F. Baker, J. Burkey, S. T. Crooke and R. M. Crooke, Antisense oligonucleotide inhibition of apolipoprotein C-III reduces plasma triglycerides in rodents, nonhuman primates, and humans, *Circ. Res.*, 2013, **112**, 1479–1490.

6 M. Matsukura, K. Shinozuka, G. Zon, H. Mitsuya, M. Reitz, J. S. Cohen and S. Broder, Phosphorothioate analogs of oligodeoxynucleotides: inhibitors of replication and cytopathic effects of human immunodeficiency virus., *Proc. Natl. Acad. Sci. U.S.A.*, 1987, **84**, 7706–7710.

7 R. I. Hara, T. Saito, T. Kogure, Y. Hamamura, N. Uchiyama, Y. Nukaga, N. Iwamoto and T. Wada, Stereocontrolled Synthesis of Boranophosphate DNA by an Oxazaphospholidine Approach and Evaluation of Its Properties, *J. Org. Chem.*, 2019, **84**, 7971–7983.

8 T. Yamada, N. Okaniwa, H. Saneyoshi, A. Ohkubo, K. Seio, T. Nagata, Y. Aoki, S. Takeda and M. Sekine, Synthesis of 2'-O-[2-(N-Methylcarbamoyl)ethyl]ribonucleosides Using Oxa-Michael Reaction and Chemical and Biological Properties of Oligonucleotide Derivatives Incorporating These Modified Ribonucleosides, *J. Org. Chem.*, 2011, **76**, 3042–3053.

9 M. Manoharan, 2'-Carbohydrate modifications in antisense oligonucleotide therapy: importance of conformation, configuration and conjugation, *Biochim. Biophys. Acta*, 1999, **1489**, 117-130.

10 A. Yahara, A. R. Shrestha, T. Yamamoto, Y. Hari, T. Osawa, M. Yamaguchi, M. Nishida, T. Kodama and S. Obika, Amido-Bridged Nucleic Acids (AmNAs): Synthesis, Duplex Stability, Nuclease Resistance, and in Vitro Antisense Potency, *ChemBioChem*, 2012, **13**, 2513–2516.

11 S. K. Singh, A. A. Koshkin, J. Wengel and P. Nielsen, LNA (locked nucleic acids): synthesis and high-affinity nucleic acid recognition, *Chem. Commun.*, 1998, 455–456.

12 X.-H. Liang, W. Shen, H. Sun, G. A. Kinberger, T. P. Prakash, J. G. Nichols and S. T. Crooke, Hsp90 protein interacts with phosphorothioate oligonucleotides containing hydrophobic 2'-modifications and enhances antisense activity, *Nucleic Acids Res.*, 2016, **44**, 3892–3907.

13 W. Shen, C. L. De Hoyos, M. T. Migawa, T. A. Vickers, H. Sun, A. Low, T. A. Bell, M. Rahdar, S. Mukhopadhyay, C. E. Hart, M. Bell, S. Riney, S. F. Murray, S. Greenlee, R. M. Crooke, X. Liang, P. P. Seth and S. T. Crooke, Chemical modification of PS-ASO therapeutics reduces cellular protein-binding and improves the therapeutic index, *Nat. Biotechnol.*, 2019, **37**, 640–650.

14 G. Vasquez, G. C. Freestone, W. B. Wan, A. Low, C. L. De Hoyos, J. Yu, T. P. Prakash, M. E. Østergaard, X. Liang, S. T. Crooke, E. E. Swayze, M. T. Migawa and P. P. Seth, Site-specific incorporation of 5′-methyl DNA enhances the therapeutic profile of gapmer ASOs, *Nucleic Acids Res.*, 2021, **49**, 1828–1839.

15 T. Yoshida, K. Morihiro, Y. Naito, A. Mikami, Y. Kasahara, T. Inoue and S. Obika, Identification of nucleobase chemical modifications that reduce the hepatotoxicity of gapmer antisense oligonucleotides, *Nucleic Acids Research*, 2022, **50**, 7224–7234.

16 A. J. Pollak, L. Zhao, and S. T. Crooke, Characterization of cooperative PS-oligo activation of human TLR9, *Mol. Ther. Nucleic Acid,* 2023, **33,** 832-844.

17 M. T. Migawa, W. Shen, W. B. Wan, G. Vasquez, M. E. Oestergaard, A. Low, C. L. De Hoyos, R. Gupta, S. Murray, M. Tanowitz, M. Bell, J. G. Nichols, H. Gaus, X. Liang, E. E. Swayze, S. T. Crooke and P. P. Seth, Site-specific replacement of phosphorothioate with alkyl phosphonate linkages enhances the therapeutic profile of gapmer ASOs by modulating interactions with cellular proteins, *Nucleic Acids Res.*, 2019, **47**, 5465–5479.

18 N. Oka, M. Yamamoto, T. Sato and T. Wada, Solid-Phase Synthesis of Stereoregular Oligodeoxyribonucleoside Phosphorothioates Using Bicyclic Oxazaphospholidine Derivatives as Monomer Units, *J. Am. Chem. Soc.*, 2008, **130**, 16031–16037.

19 N. Oka, T. Kondo, S. Fujiwara, Y. Maizuru and T. Wada, Stereocontrolled Synthesis of Oligoribonucleoside Phosphorothioates by an Oxazaphospholidine Approach, *Org. Lett.*, 2009, **11**, 967–970.

20 L. Arrico, C. Stolfi, I. Marafini, G. Monteleone, S. Demartis, S. Bellinvia, F. Viti, M. McNulty, I. Cabani, A. Falezza and L. Di Bari, Inhomogeneous Diastereomeric Composition of Mongersen Antisense Phosphorothioate Oligonucleotide Preparations and Related Pharmacological Activity Impairment, *Nucleic Acid Ther.*, 2022, **32**, 312–320.

21 E. B. McElroy, R. Bandaru, J. Huang and T. S. Widlanski, Synthesis and Physical Properties of Sulfonamide-Containing Oligonucleotides, *Bioorg. Med. Chem. Lett.*, 1994, **4**, 1071–1076.

22 V. Korotkovs, L. F. Reichenbach, C. Pescheteau, G. A. Burley and R. M. J. Liskamp, Molecular Construction of Sulfonamide Antisense Oligonucleotides, *J. Org. Chem.*, 2019, **84**, 10635–10648.

23 Y. Masaki, A. Tabira, S. Hattori, S. Wakatsuki and K. Seio, Insertion of a methylene group into the backbone of an antisense oligonucleotide reveals the importance of deoxyribose recognition by RNase H, *Org. Biomol. Chem.*, 2022, **20**, 8917–8924.

24 J. Huang, E. B. McElroy and T. S. Widlanski, Synthesis of Sulfonate-Linked DNA, *J. Org. Chem.*, 1994, **59**, 3520–3521.

25 a) G. Blotny, A new, mild preparation of sulfonyl chlorides, *Tetrahedron Lett., 2003,* **44***,* 1499-1501.; b) T. Tomori, K, Uekusa, A. Koyama, T. Kanagawa, Y. Masaki and K. Seio, Synthesis of 2'-O-[3-(N-methylsulfamoyl)propan-1-yl]ribothymidine as a potentially applicable 2′-modified nucleoside for antisense oligonucleotides, *Bioorg. Med. Chem.*, *2022*, **73**, 117002.

26 A. R. Khomutov, A. S. Shvetsov, J. J. Vepsäläinen and A. M. Kritzyn, Novel acid-free cleavage of N-(2-hydroxyarylidene) protected amines, *Tetrahedron Lett.*, 2001, **42**, 2887–2889.

27 R. Eisenhuth and C. Richert, Convenient Syntheses of 3'-Amino-2',3'-dideoxynucleosides, Their 5'-Monophosphates, and 3'-Aminoterminal Oligodeoxynucleotide Primers , *J. Org. Chem.*, 2009, **74**, 26–37.

28 N. Papargyri, M. Pontoppidan, M. R. Andersen, T. Koch and P. H. Hagedorn, Chemical Diversity of Locked Nucleic Acid-Modified Antisense Oligonucleotides Allows Optimization of Pharmaceutical Properties, *Mol. Ther. Nucleic Acids*, 2020, **19**, 706–717.

29 K. J. Fettes, N. Howard, D. T. Hickman, S. A. Adah, M. R. Player, P. F. Torrence and J. Micklefield, Replacement of the phosphodiester linkage in DNA with sulfamide and 3'-N-sulfamate groups, *Chem. Commun.*, 2000, 765–766.

30 K. J. Fettes, N. Howard, D. T. Hickman, S. Adah, M. R. Player, P. F. Torrence and J. Micklefield, Synthesis and nucleic-acid-binding properties of sulfamide- and 3'-N-sulfamate-modified DNA, *J. Chem. Soc., Perkin Trans. 1*, 2002, 485–495.

31 C. Moriou, M. Thomas, M.-T. Adeline, M.-T. Martin, A. Chiaroni, S. Pochet, J.-L. Fourrey, A. Favre and P. Clivio, Crystal Structure and Photochemical Behavior in Solution of the 3′-N-Sulfamate Analogue of Thymidylyl(3′-5′)thymidine, *J. Org. Chem.*, 2007, **72**, 43–50.

32 D. A. Shuman, M. J. Robins and R. K. Robins, Synthesis of nucleoside sulfamates related to nucleocidin, *J. Am. Chem. Soc.*, 1970, **92**, 3434–3440.

33 M. Nowotny, S. A. Gaidamakov, R. Ghirlando, S. M. Cerritelli, R. J. Crouch and W. Yang, Structure of human RNase H1

complexed with an RNA/DNA hybrid: insight into HIV reverse transcription, *Mol. Cell*, 2007, **28**, 264–276.

Data availability

The data supporting this article have been included as part of the Supplementary Information.